Compressing an elliptic vortex: transition to turbulence by tumble breakdown

By Fabien S. Godeferd[1], Nagi N. Mansour[2] AND Claude Cambon[1]

1. Motivations and objectives

Stability of the elliptic vortex attracted interest in the past decade. Cambon (1982), and Cambon, Teissèdre and Jeandel (1985) have studied the stability of such flows with spatially uniform velocity gradient, and have provided RDT solutions for a wide range of the parameter S/Ω (where the strain rate S and the vorticity 2Ω define the velocity gradient matrix). The range studied included those of hyperbolic streamlines (strain dominated, $S/\Omega > 1$), linear streamlines (simple shear, $S/\Omega = 1$), and elliptical streamlines (vorticity dominated, $S/\Omega < 1$). The latter class has more recently attracted interest and several studies appeared (Pierrehumbert 1986, Bayly 1986, Craik and Criminale 1986). These studies will be collectively referred to as PBCC. Recent review of the subject of instability of elliptic flows and significant progress in this area can be found in Waleffe (1990).

Background linear instability (in the elliptic core of actual eddies) was shown to be the active mechanism in several complex transitional and turbulent flows, including mixing layers, wakes, trailing vortices, etc. This was the primary motivation for the study of stability and transition to turbulence using Direct Numerical Simulations (DNS) by Blaisdell and Shariff (1994) and by Lundgren and Mansour (1996) for a confined elliptic vortex. Linear stability analysis of an unbounded elliptic vortex, stretched along its axis, was analytically performed by Le Dizès, Rossi and Moffat (1996, hereafter referred to as L-DRM). The case of a circular unbounded vortex, periodically compressed along its axis, was studied by Mansour & Lundgren (1990). This study showed that the flow displays a parametric instability due to the interaction between vorticity and periodic compression, *in the absence of ellipticity, or additional weak planar strain.* The present paper shares the motivations of these previous works regarding fundamental aspects of transition to turbulence, and is particularly connected to the latter three papers. Another specific motivation, however, comes from the dynamics of turbulence in reciprocating engines, as presented hereafter.

During the compression stroke, both *swirl* (axis parallel to the direction of compression) and *tumble* (axis perpendicular to the direction of compression) mean vortices are present. These vortices evolve in different ways. The swirling motion is stabilized by the compression (even if potential instabilities exist, as shown by Mansour & Lundgren 1990), whereas the tumble motion (created by the off-set

1 LMFA UMR 5509 – École Centrale de Lyon – France
2 NASA Ames Research Center

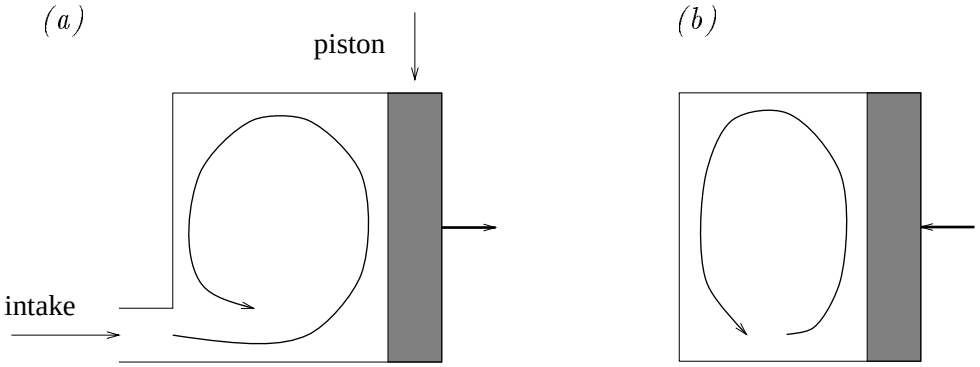

FIGURE 1. Sketch (a) of the generation of the tumble by injection in the experiment, (b) and the following compression of the tumble.

from the symmetry axis of the intake-valve jet) is often observed to break down. Such a breakdown is desirable near the end of the compression stroke, since it could enhance turbulence and mixing at the beginning of the combustion stroke. This problem has motivated research projects which involve both an experimental study of a compressed tumble (Marc *et al.*, 1996) and a related numerical approach using single-point closures (Leroy and Le Penven, 1996). A sketch of the experimental setup is shown in Fig. 1.

The three-dimensional character of the disturbances within a parametric instability of the elliptical-type was not addressed in previous studies.

2. Linear stability and RDT approach to the unbounded flow

Rapid Distortion Theory (RDT) and linear stability analysis start from the same equations in the case of background (or mean) flow with uniform velocity gradient. The background (mean) velocity field is a solution of the Euler equations. The disturbance (or fluctuating) field can be sought under the form of time-dependent three-dimensional Fourier modes. On the one hand, considering a single-mode disturbance field, the solutions of the linearized equations are exact solutions (as pointed out by Craik and Criminale, 1986). On the other hand, RDT considers a sum over all of the Fourier modes, nonlinear coupling terms are neglected through the RDT assumption. This approach has the advantage that the computation of statistics is possible. Statistical homogeneity, in the sense of ensemble average, for the disturbance field is preserved by the space-uniform mean distortion, and, in turn, is consistent with the decoupling of the 'mean' flow (solution of Euler equations) in the absence of feedback from the Reynolds stress gradient.

2.1 The background flow

In three dimensions, we are concerned with the following mean velocity gradient matrix:

$$U_{i,j} \rightarrow \begin{pmatrix} -S(t) & -\Omega(t) & 0 \\ \Omega(t) & 0 & 0 \\ 0 & 0 & 0 \end{pmatrix} \qquad (1)$$

where the mean velocity field $U_i = \lambda_{ij}(t)x_j$ is a superposition of a pure compression flow of rate $S(t)$ and a pure rotation flow of angular velocity $\Omega(t)$, or vorticity $2\Omega(t)$, where t is the time variable. The compression is chosen along the axis 1, and the vorticity vector is along the axis 3, in agreement with a 'tumble' flow pattern. The compression rate S is calculated given a uniform lengthscale variation law in the x_1 direction

$$L(t)/L(0) = \frac{(1+1/r)}{2} + \frac{(1-1/r)}{2}\cos(2\omega t) \tag{2}$$

so that

$$S(t) = -\dot{L}/L \quad \text{and} \quad \Omega(t) = \Omega_0 L(0)/L(t), \tag{3}$$

where $\dot{\{\}}$ indicates the time derivative. The latter equation ensures that the mean velocity field is a solution of the Euler equations and reflects the conservation of angular momentum. The compression law (2), or equivalently the volumetric law, is roughly similar to the one in an actual engine, where r is the maximum volumetric ratio which is reached when $2\omega t = \pi$ (see also Mansour & Lundgren 1990). Hence the three parameters r, ω, and Ω_0 completely characterize the background flow. Of course, different $L(t)$-laws can be used in Eqs. (3) and (1) if necessary.

Elliptic stream-functions corresponding to Eq. (1) are more classically formulated in a system where the axes are rotated ($\alpha = \pi/4$) around the x_3 direction, so that

$$U_{i,j} \rightarrow \begin{pmatrix} -S/2 & -S/2-\Omega & 0 \\ -S/2+\Omega & -S/2 & 0 \\ 0 & 0 & 0 \end{pmatrix} \tag{1'}$$

and the extra-diagonal part is the same as the one considered by PBCC, but with time-dependent coefficients. Splitting the matrix into trace and deviator, one finds

$$\begin{pmatrix} -S/3 & 0 & 0 \\ 0 & -S/3 & 0 \\ 0 & 0 & -S/3 \end{pmatrix} + \begin{pmatrix} -S/6 & -S/2-\Omega & 0 \\ -S/2+\Omega & -S/6 & 0 \\ 0 & 0 & S/3 \end{pmatrix} \tag{1''}$$

in which the trace-free (incompressible) part is similar to the one considered by L-DRM.

2.2 Linear stability and RDT

After splitting the velocity and pressure field into a background (capital letters) and a disturbance part (lower case letters), namely $U_i + u_i$ and $P + p$, the linearized equations for the disturbances are solved using three-dimensional Fourier modes in the coordinate system that follows the background field. Note that this approach is Lagrangian with respect to the mean trajectories. With the method used by Cambon and coworkers since the early eighties (see Cambon *et al.*, 1994, for an up-to-date presentation in English), the linear problem amounts to solving a system of two coupled differential equations for two solenoidal components of the disturbance velocity field, along trajectories in Fourier space. The numerical code (denoted MITHRA) is basically the same as the one used by Cambon (1982) and Cambon

et al. (1985) to study the effects of the elliptical flow instability on the turbulence statistics.

The linear solutions are computed under the form of two matrices:

- The first one is the Lagrangian displacement tensor $F_{ij}(t,0) = \partial x_i/\partial X_j$ which characterizes the background flow trajectories in physical and spectral space, or:

$$x_i = F_{ij}(t,0)X_j \qquad k_i = F^{-1}_{ji}(t,0)K_j \qquad k_i x_i = K_i X_i \tag{4}$$

  where space coordinates and wavevectors in capital letters stand for Lagrangian ones with respect to the mean. Similar formalism used in DNS is often referred to as 'Rogallo space' (Rogallo, 1981).

- The second one, denoted $g_{\alpha\beta}(\boldsymbol{k}/k,t,0)$, characterizes the linear inviscid response of the disturbance field. The number of components is minimal (rank-two matrix), when taking into account the solenoidal property. This is equivalent to the fact that the velocity Fourier amplitude vector lies in the plane normal to the wave vector. More details are summarized in the appendix.

These two matrices completely characterize the inviscid linear stability problem. In addition, the viscous contribution can be obtained easily, as recently recovered by Landman and Saffman (1987) in the particular case of the elliptic flow. The statistics of homogeneous turbulence can be computed as well, given an initial form for the velocity statistical moments (e.g. isotropic), as has been done in classic RDT for over forty years (Batchelor and Proudman, 1954).

Compared to previous linear stability and RDT studies, the case of the compressed tumble presents some original features as follows:

- The background flow is compressible. An important parameter is the volumetric ratio $J = \det \boldsymbol{F}$, equal to $L(t)/L(0)$ for a one-dimensional compression. This brings only a few changes since the disturbance field is solenoidal, meaning that we deal here with *compressed,* but not compressible turbulence. This type of approximation is justified at low Mach number, as discussed by Mansour & Lundgren (1990). Note that the spherical part of the mean velocity gradient matrix, as in Eq. $(1'')$, could be removed from consideration by a rescaling of the disturbance field (Cambon *et al.*, 1992).

- The ellipticity and vorticity are continuously varying in a very different way from that in the study by L-DRM, even though axial stretching and the related increase of the axial vorticity were similar, looking at the incompressible part of $(1'')$. In the compressed case addressed by Mansour & Lundgren, the axial vorticity was steady and there was no ellipticity.

Typical results for stability analysis are presented as a function of the angular distribution of the matrix $\boldsymbol{g}$ in wave-space. Since, indeed, in the unbounded inviscid case, it depends only on the orientation of the wave vector and not on its modulus.

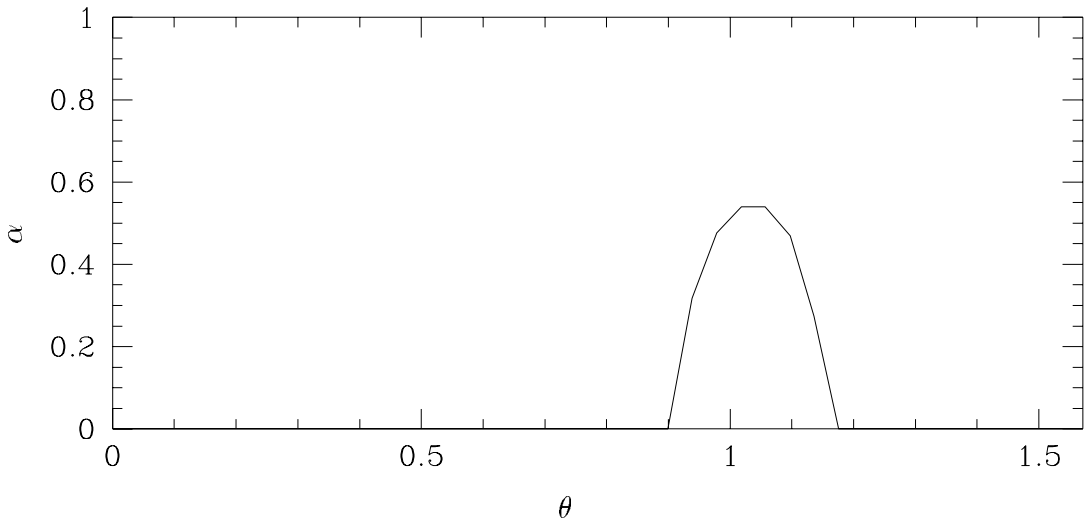

FIGURE 2. Elliptic vortex: Floquet parameter α as a function of the orientation θ of the Fourier mode $\boldsymbol{k}$. The peak value is located around $\theta = \pi/3$ with a maximum close to 9/16 (see e.g. Waleffe, 1990).

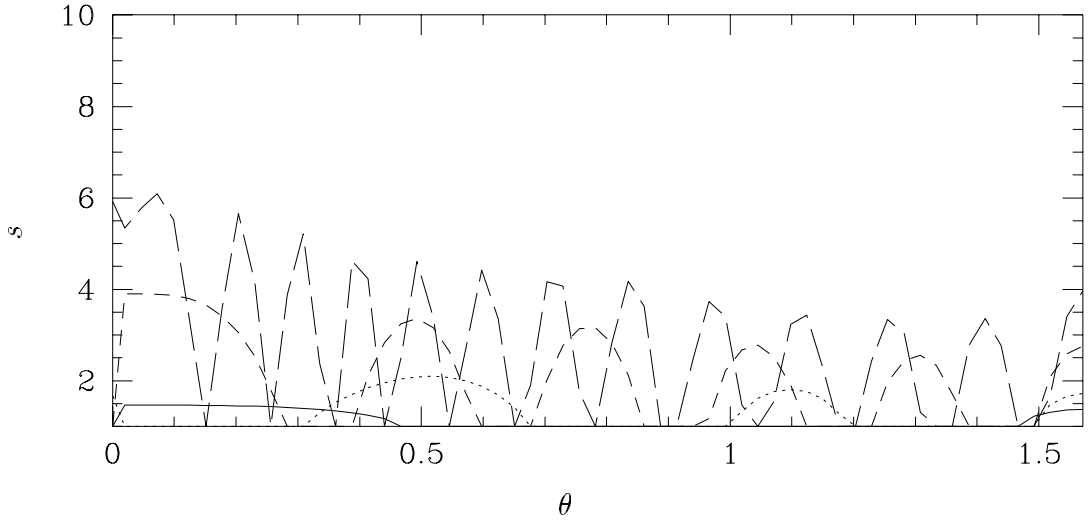

FIGURE 3. Same as Fig. 6 with $\Omega_0 = 100$.

Figure 2 shows the case of the classic elliptic instability (the diagonal terms are not present in Eq. (1′)) and S and Ω are chosen constants. The maximum eigenvalue s of $\boldsymbol{g}$ is computed after a period $T = 2\pi/\sqrt{\Omega^2 - S^2}$, which with respect to $\boldsymbol{F}$ corresponds to the time needed for closing elliptic trajectories. Under the form of a non-dimensional Floquet coefficient α defined from $s = \exp(\alpha ST)$, the classic distribution is recovered when the angle of $\boldsymbol{K}$ with the axis of the vortex (x_3) varies from 0 to $\pi/2$ at $K_1 = 0$. Accordingly, a single peak of instability emerges around $\pi/3$, with a maximum close to 9/16 (Waleffe, 1989, Cambon *et al.*, 1994).

Figures 3, 4, and 5 show the corresponding case for the compressed tumble at

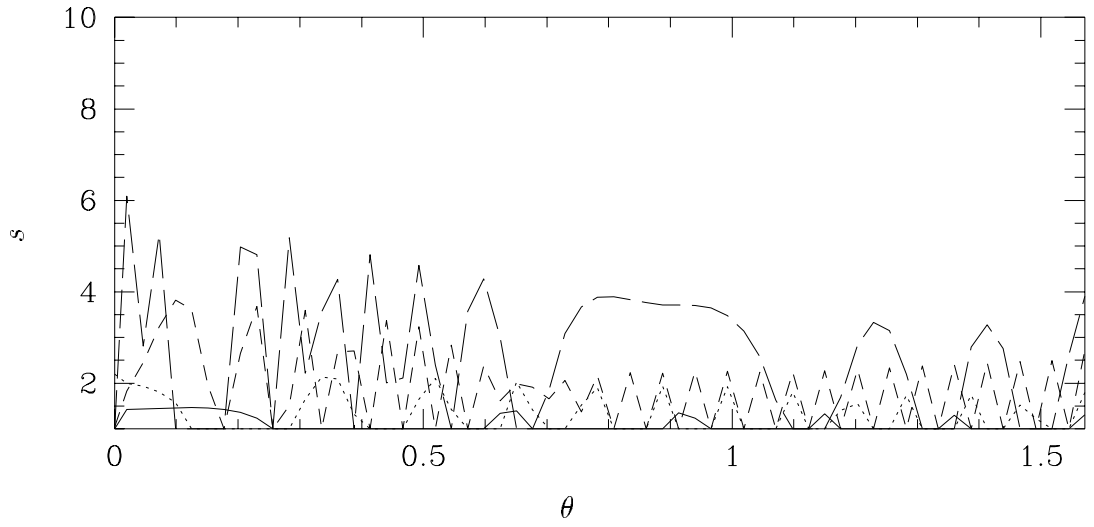

FIGURE 4. Same as Fig. 6 with $\Omega_0 = 500$.

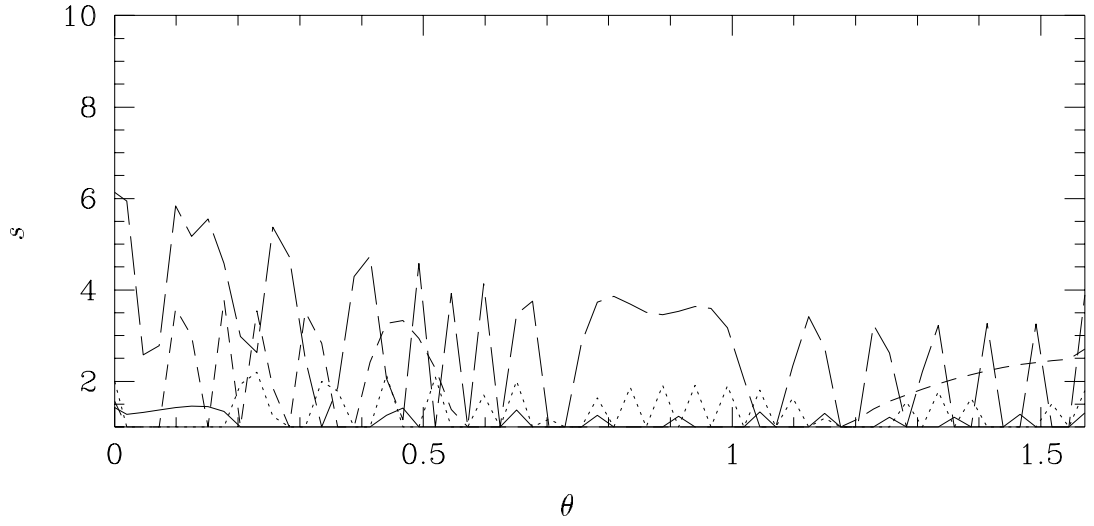

FIGURE 5. Same as Fig. 6 with $\Omega_0 = 1000$.

four different non-dimensional times (or crank angles) ($2\omega t = \pi/4,\ \pi/2,\ 3\pi/2,\ \pi$ in Eq. (2)). The tumble is assumed to be circular at the initial time since $S = 0$, and to have the maximum aspect ratio r at the final time. A convenient 'realistic' choice of parameters in the context of reciprocating engines is $r = 10$, $2\omega = 52\,s^{-1}$, with different values for $\Omega_0 = 100$ (Fig. 3), $\Omega_0 = 500$ (Fig. 4), $\Omega_0 = 1000$ (Fig. 5).

Compared to the case of the stationary elliptic vortex where a single instability peak is exhibited and to the elongated elliptic vortex (Le Dizès *et al.,* 1996) where the instability growth is inhibited by a sufficiently rapid stretching rate, the present results are completely different and particularly important regarding a possible 'explosive' instability. The case of pure compression ($\Omega_0 = 0$) is also shown in Fig. 6 to contrast with the tumble case. The only case where a number of instability

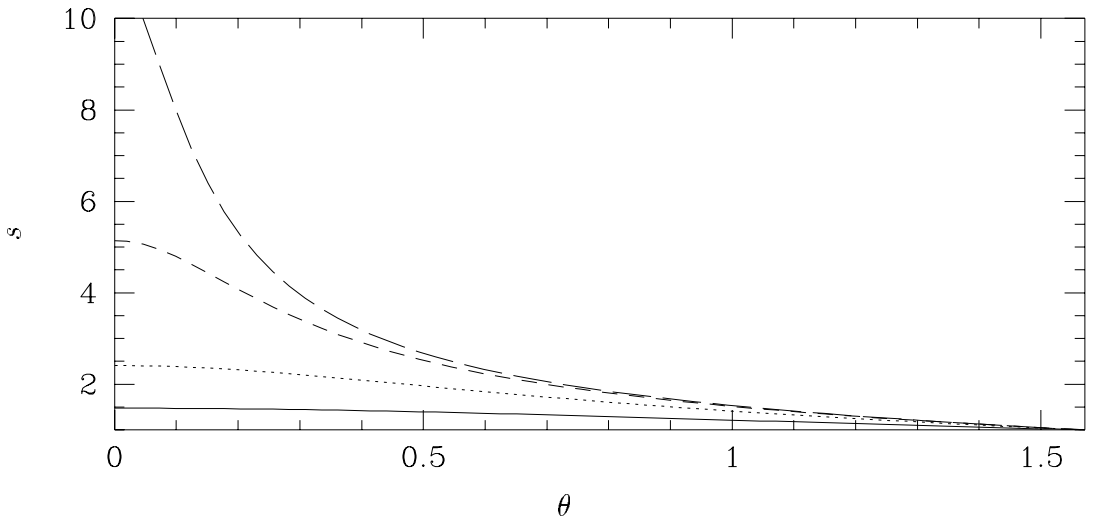

FIGURE 6. Maximum eigenvalue s of the amplification matrix $\boldsymbol{g}$ for different orientations θ of the Fourier mode $\boldsymbol{k}$. This case with no vorticity $\Omega_0 = 0$, at different crank angles: ——— , $\omega t = \pi/4$; ····· , $\omega t = \pi/2$; - - - - , $\omega t = 3\pi/4$; — — — — , $\omega t = \pi$.

bands were found is the periodically compressed swirl flow (Mansour & Lundgren 1990), but our results display an unexpected number of unstable thin bands. The most general analytical results for the steady elliptical flow and the periodically compressed swirl flow, which are based on Hill's equations, are summarized in the appendix.

Figure 7 shows that the kinetic energy history is weakly affected by the complex instability distribution. The growth of the turbulent kinetic energy reflects the scrambling effect of rotation, which diminishes the Reynolds stress anisotropy and, therefore, the energy production. As a result, the energy growth rate is reduced by the presence of rotation.

3. Future plans

Linear analysis has shown that tumble will play an important role in the evolution of turbulence which is subjected to compression. We plan to carry out a DNS of this flow. The DNS will follow the approach of Lundgren and Mansour (1996) where a confined elliptic flow was studied. The velocity field will be expanded in sine and cosine series in x- and y-directions and Fourier series in the z-direction. The y-coordinate will move in time following a one-dimensional compression.

Appendix A. A short review of the analytical works using Hill's equations

In this appendix we develop the linearized equations for a general uniform deformation tensor and summarize the various studies used to analyze the instability of flows under rotation and strain.

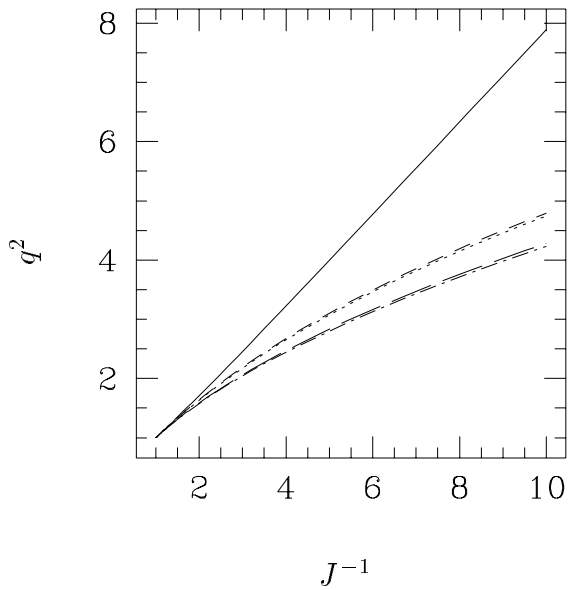

FIGURE 7. Evolution of the normalized kinetic energy for the compressed tumble vortex, as a function of the volumetric ratio J^{-1}, with $J^{-1} = 10$ at the end of the compression. ——— , $\Omega_0 = 0$; ····· , $\Omega_0 = 10$; - - - - , $\Omega_0 = 100$; – – – – , $\Omega_0 = 500$; —·— , $\Omega_0 = 1000$.

A.1. Linear equations and generic solutions for disturbances

In the presence of a background (or mean) velocity field $U_i = U_{i,j}(t)x_j \equiv \lambda_{ij}(t)x_j$, possibly divergent ($U_{l,l} = \lambda_{ll} = \dot{J}/J$), linearized equations for the amplitudes of velocity disturbances are

$$\dot{\hat{u}}_i + \lambda_{ll}\hat{u}_i + \nu k^2 \hat{u}_i = -\left(\delta_{il} - 2\frac{k_i k_l}{k^2}\right)\lambda_{lj}\hat{u}_j \qquad (A.1)$$

where velocity and pressure disturbances are expressed in terms of 3D Fourier modes, or

$$[u_i, p] = [\hat{u}_i(\boldsymbol{k}, t), \hat{p}(\boldsymbol{k}, t)]e^{i\boldsymbol{k}.\boldsymbol{x}} ,$$

and the wavevector $\boldsymbol{k}$ is considered as time-dependent, following the characteristic curves (second Eq. (4)), that are solutions of

$$\dot{k}_i = -\lambda_{ji}k_j \qquad \text{and} \qquad k_i(t=0) = K_i . \qquad (A.2)$$

The overdot $\dot{\{\}}$ denotes a time derivative *at fixed* $\boldsymbol{K} = \boldsymbol{k}(t=0)$, which is similar to the substantial derivative in physical space. Eq. (A.1) is valid for any unbounded *solenoidal* velocity disturbance field ($k_i\hat{u}_i = 0$), in agreement with the closed expression

$$p' = k_j\lambda_{jl}\hat{u}_l \qquad (A.3)$$

for a term proportional to the Fourier transform of the pressure Laplacian. The background field is a particular solution of the Euler equations if $\dot{\boldsymbol{\lambda}} + \boldsymbol{\lambda}^2$ is a symmetric tensor, or equivalently if the mean vorticity obeys the Helmholtz equations. Without lack of generality, Eqs. (A.1) and (A.2) for the initial value problem have solutions of the form

$$k_i = M_{ij}(t,0)K_j \quad \text{with} \quad \boldsymbol{M} = \boldsymbol{F}^{-1} \quad \text{and} \quad M_{ij}(t=0,0) = F_{ij}(t=0,0) = \delta_{ij} \tag{A.4}$$

and

$$\hat{u}_i(\boldsymbol{k},t) = G_{ij}(\boldsymbol{k}/k,t,0)\exp\left[-\nu V_{ln}(\boldsymbol{k}/k,t,0)k_l k_n\right]\hat{u}_j(\boldsymbol{K},0) \quad \text{with} \quad G_{ij}(t=0) = \delta_{ij} - K_i K_j/K^2 \tag{A.5}$$

where the matrices $\boldsymbol{F}$, as in Eq. (4) (or $\boldsymbol{M}$), $\boldsymbol{G}$, and $\boldsymbol{V}$ are deterministic and can be tabulated once for all for a given background velocity field. For the sake of simplicity, the exponential viscous factor will no longer be considered in the following. The two-time argument $(t,0)$ reflects that we are concerned with linear transfer operators from an initial $(t = 0)$ state to an instantaneous one, as for Green's functions. Of course $\boldsymbol{F}$ and $\boldsymbol{G}$ are the basis for the most general linear stability analysis. The main difficulty comes from the implicit time-dependence of the orientation of $\boldsymbol{k}$ in the linear system for $\boldsymbol{G}$, or equivalently in inviscid Eq. (A.1). Optional subsequent prediction of statistics (e.g. $< \hat{u}_i^* \hat{u}_j >$) is obtained in terms of initial statistics and products of $\boldsymbol{G}$ matrices.

A final reduction of the number of dependent deterministic functions that generate the linear solutions is to use a rank-2 matrix (the $\boldsymbol{g}$ matrix) rather than $\boldsymbol{G}$, considering only the two nonzero components $(\hat{\varphi}^\alpha, \alpha = 1,2)$ of $\hat{u}_i$ in a plane normal to $\boldsymbol{k}$, in accordance with the solenoidal property. The linear combinations $\hat{\varphi}^2 \pm i\hat{\varphi}^1$ are the amplitudes of the 'helical modes', useful in any problem involving rotation.

In addition to analytical solutions discussed in previous works, the code MITHRA can numerically solve the linear problem in the most general way as follows. The input is the initial mean vorticity vector $2\Omega_i(t=0) = \epsilon_{ijk}\lambda_{kj}(t=0)$, the time-dependent symmetric part $\lambda_{ij}(t)+\lambda_{ji}(t)$, and data about discretisation of the initial wavevector. In addition, one can introduce given initial statistical velocity moments. The actual time evolution for the eventually unsteady vortical part of the mean, in agreement with Helmholtz equation, is automatically ensured, and $\boldsymbol{F}$, $\boldsymbol{V}$ and $\boldsymbol{g}$ are numerically computed using a fourth-order Runge-Kutta method. Given a periodic history of $\boldsymbol{F}$, hence a periodic wavevector motion as considered below, diagonalization of $\boldsymbol{g}$ after a time-period yields values and spectral distributions of the Floquet parameter, but this is only a very peculiar application of MITHRA.

Hill's equations considered in subsequent subsections can be found starting from a special set of two components that generates $\hat{u}_i$ for the solenoidal velocity field. These two components are similar to the $\hat{\varphi}^\alpha, \alpha = 1,2$ addressed by Cambon and coworkers (used in MITHRA for computing $\boldsymbol{g}$), and also proportional to the amplitudes of the Laplacian of vertical velocity ($\nabla^2 u_3$ used in classic Orr-Sommerfeld equation) and vertical vorticity ($\omega_3 = \epsilon_{3ij}u_{j,i}$ used in classic Squires equation).

A.2. The basic elliptical flow

The planar ($\alpha, \beta = 1, 2$) background flow is characterized by

$$\lambda_{\alpha\beta} \rightarrow \begin{pmatrix} 0 & S_0 - \Omega_0 \\ S_0 + \Omega_0 & 0 \end{pmatrix} \qquad (A.6)$$

Starting from Eqs. (A.1) and (A.2) a linear system for $\hat{u}_3$ and p' (Eq. (A.3)) is found,

$$\dot{(k^2 p')} = 2(S_0^2 - \Omega_0^2) k^2 k_3 \hat{u}_3$$

and

$$k^2 \dot{(\hat{u}_3)} = 2 k_3 p' \ .$$

By elimination of p' in the previous system, one finds a second order ODE:

$$\ddot{(k^2 \hat{u}_3)} = 4[-\Omega_0^2 k_3^2 + S_0^2 k^2 + S_0 \Omega_0 (k_2^2 - k_1^2)] \hat{u}_3 \qquad (A.7)$$

which is valid for any case (hyperbolic $S_0 > \Omega_0$, pure shear $S_0 = \Omega_0$, and elliptic $S_0 < \Omega_0$) addressed by Cambon and coworkers. In the elliptical case ($S_0 < \Omega_0$), the motion of $\boldsymbol{k}$ is periodic, in agreement with $\ddot{F}_{\alpha\beta} = (S_0^2 - \Omega_0^2) F_{\alpha\beta}$ so that $\ddot{k}_i = (S_0^2 - \Omega_0^2)(k_i - k_3 \delta_{i3})$. In this case only, the above Eq. (A.7) is the specific Hill's equation addressed by Waleffe (1990), up to a slightly different choice (not K_i, $i = 1, 2, 3$ as in (4) and (A2)) to initialize $\boldsymbol{k}$. When the specific periodic motion of $\boldsymbol{k}$ is accounted for, the above equation is parameterized by the two angular-dependent (in terms of the orientation of $\boldsymbol{K}$) parameters a and c below that define the configuration plane in which to plot isovalues of the Floquet parameter. This is used to have a complete and synoptic representation of the linear stability problem. Waleffe found

$$(1 - a\cos(2\phi))\, \ddot{Z} + \left(c^2 - 4a\cos(2\phi)\right) Z = 0$$

with $Z = k^2 \hat{u}_3$, $\phi = \sqrt{\Omega_0^2 - S_0^2}(t - t_0)$, and he plotted the neutral curve in the (a, c)-plane.

A.3. The periodically compressed circular (swirl) flow

The *compressing* background flow is given by

$$\lambda_{ij} = \begin{pmatrix} 0 & -\Omega_0 & 0 \\ \Omega_0 & 0 & 0 \\ 0 & 0 & S(t) \end{pmatrix}$$

where the axial strain-rate $S = \dot{L}/L$ is given by a periodic law, similar to (2) for $L(t)$, and the vorticity is constant since the mean flow is compressible (no amplification by vortex stretching). In this case, the two relevant components used by Mansour & Lundgren are proportional to horizontal (or vertical) divergence ($\Phi = k_1 \hat{u}_1 + k_2 \hat{u}_2 = -k_3 \hat{u}_3$) and vertical axial vorticity ($\Psi = k_1 \hat{u}_2 - k_2 \hat{u}_1$). The corresponding Hill's

equation is finally found by eliminating Ψ, and working with $\xi = L^2(t)k^2(t)\Phi$, so that

$$\left[1 - a\sin(2t^*) + 0.5\eta a \sin^2(2t^*)\right] \ddot{\xi} = -\sigma^2 \xi$$

where $t^* = \omega t$ is the non-dimensional time and $\eta = (r-1)/(r+1)$, as in (2). In terms of the two angular parameters that parameterize this Hill's equation, namely $\sigma = 2(\Omega_0/\omega)\cos\theta$ and $a = 2\eta \sin^2\theta$, the relevant representation plane was found in which isovalues of the Floquet parameter were numerically plotted, not only the neutral curves. Different instability bands were shown in the (a, σ)-plane that correspond to different instability bands in terms of θ, as shown in the present Figures 2-6. In order to contrast the results in Fig. 1 (Mansour & Lundgren) and the results delivered by MITHRA, we have computed a typical RDT history of $\boldsymbol{g}$ in the same conditions.

For a compression ratio $r = 8$ and a swirl ratio $\Omega_0/\omega = 2$, the parabolic dashed line, which gives in the (a, σ)-plane the variation in θ at fixed compression and swirl ratios (the Mansour-Lundgren Fig. 1), predicts three unstable angular bands. These bands are accurately recovered when looking at the angular θ distribution of the maximum eigenvalue of $\boldsymbol{g}$ after a period ($t = T = \pi/\omega$).

A.4. Relevance of the Floquet analysis to the compressed tumble case

The mean flow gradient matrix corresponding to Eq. (1-3) yields a more complex problem than the two cases reported above. Even if it were possible to derive a unique second order ODE from the two-equations linear system (from A.1) in terms of either

- $(\hat{\varphi}^1, \hat{\varphi}^2)$ (Cambon and coworkers),
- $(\hat{u}_3, p')$ (Waleffe) or
- $(-k_3\hat{u}_3, -i\hat{\omega}_3)$ (Mansour & Lundgren),

the specific time dependence induced by the motion of $\boldsymbol{k}$ would remain analytically unknown in the coefficients of such a second order ODE. Even the solution (4) of Eq. (A.2) cannot be simply expressed. In fact k_1 and k_2 are themselves governed by a Hill- type equation!).

Regarding, now, the Floquet problem, which can always be numerically treated by computing the $\boldsymbol{g}$-angular distribution after a period, we obtained the following preliminary information:

- The angular distribution after a complete period depends on the initial phase or initial crank angle when using either (2) or the compression history of Mansour-Lundgren compression law. No instability is found, reflecting a complete reversibility of the $\boldsymbol{g}$ history, when using (2) (where $\dot{L} = 0$ initially), whereas a number of instability peaks is found when starting from an extremum of $\dot{L}$, as Mansour-Lundgren did.
- The distribution of instability peaks obtained at the end of the compression stroke (Figs. 2-5) has nothing to do with the distribution obtained after a complete period.

- Even if a non-periodic law is used for reaching the end of the compression stroke (e.g. a constant strain-rate and exponential decrease for $L(t)$ were checked), a 'forest' of instability peaks is still obtained, but its distribution is different from the one corresponding to (2).

This refined numerical analysis illustrates that the results from a Floquet analysis should be treated with caution since in general such an analysis is strongly dependent on the form of the compression law.

REFERENCES

Batchelor, G. K. & Proudman, I. 1954 The effect of rapid distortion on a fluid in turbulent motion. *Q. J. Mech. Appl. Maths.* **7,** 83-103.

Bayly, B. J. 1986 Three-dimensional instability of elliptical flow. *Phys. Rev. Lett.* **57,** 2160-2171.

Blaisdell, G. A. & Shariff, K. 1994 Homogeneous turbulence subjected to mean flow with elliptic streamlines. *Proceedings of the 1994 Summer Program,* Center for Turbulence Research, Stanford, CA., 355-371.

Cambon, C. 1982 Étude spectrale d'un champ turbulent incompressible soumis à des effets couplés de déformation et de rotation imposés extérieurement. *Thèse de doctorat* d'état, Université Claude Bernard-Lyon I.

Cambon, C., Benoit, J. P., Shao, L. & Jacquin, L. 1994 Stability analysis and large eddy simulation of rotating turbulence with organized eddies. *J. Fluid Mech.* **278,** 175-200.

Cambon, C., Coleman, G. N. & Mansour, N. N. 1993 Rapid distortion analysis and direct simulation of compressible homogeneous turbulence at finite Mach number. *J. Fluid Mech.* **257,** 641-665.

Cambon, C., Mao, Y. & Jeandel, D. 1992 On the application of time dependent scaling to the modelling of turbulence undergoing compression. *Eur. J. Mech. B/Fluids.* **11**(6), 683-703.

Cambon, C., Teissèdre, C. & Jeandel, D. 1985 Étude d'effets couplés de déformation et de rotation sur une turbulence homogène. *J. Méc. Théor. Appl.* **4,** 629-657.

Craik, A. D. D. & Criminale, W. O. 1986 Evolution of wavelike disturbances in shear flows: a class of exact solutions of the Navier-Stokes equations. *Proc. R. Soc. Lond. A.* **406,** 13-26.

Landman, M. J. & Saffman, P. G. 1987 The three-dimensional instability of strained vortices in a viscous fluid. *Phys. Fluids.* **30,** 2339-2342.

Le Dizès, S., Rossi, M. & Moffatt, H. K. 1996 On the three-dimensional instability of elliptical vortex subjected to stretching. *Phys. Fluids.* **8**(8), 2084-2090.

LEROY, O., LE PENVEN, L., CAMBON, C. & SCOTT, J. 1996 Combustion dans les moteurs à piston. *Rapport ARC CNRS/ECOTECH/GIE PSA-RENAULT.* Rapport 1995-96, LMFA Ecole Centrale de Lyon, France.

LUNDGREN, T. S. & MANSOUR, N. N. 1996 Transition to turbulence in an elliptic vortex. *J. Fluid Mech.* **307,** 43-62.

MANSOUR, N. N. & LUNDGREN, T. S. 1990 Three-dimensional instability of rotating flows with oscillating axial strain. *Phys. of Fluids A.* **12**(2), 2089-2091.

MARC, D., BORÉE, J., BAZILE, R., CHARNAY, G., TRINITÉ, M. & LECERF, A. 1996 Étude expérimentale modèle de l'aérodynamique interne des moteurs: cas de l'écoulement de rouleau. $5^{ème}$ *congrès francophone de vélocimétrie laser,* Rouen, France. 24-27 Sept. 1996.

PIERREHUMBERT, T. J. 1986 Universal short-wave instability of two-dimensional eddies in an inviscid fluid. *Phys. Rev. Lett.* **57,** 2157-2159.

ROGALLO, R. S. 1981 Numerical experiments in homogeneous turbulence. *NASA Tech. Mem. 81315.*

WALEFFE, F. 1989 The three-dimensional instability of a strained vortex and its relation to turbulence. *PhD thesis.* MIT.

WALEFFE, F. 1990 On the three-dimensional instability of strained vortices. *Phys. of Fluids A.* **2**(1), 76-80.